Single-photon-induced random telegraph signal in a two-dimensional multiple-tunnel-junction array

Ratno Nuryadi, Yasuhiko Ishikawa, and Michiharu Tabe*

Research Institute of Electronics, Shizuoka University, 3-5-1 Johoku, Hamamatsu 432-8011, Japan

(Received 8 September 2005; published 11 January 2006; publisher error corrected 17 January 2006)

A single-photon detection using a Si-based two-dimensional (2D) multiple-tunnel-junction field-effect transistor (FET) is reported. The single photon is detected as a random telegraph signal (RTS) in the single-hole-tunneling current regime. The frequency of RTS events depends on the light wavelength and intensity, indicating that the RTS occurs due to the single-photon absorption in the Si dots forming the 2D multijunctions. Based on a Monte Carlo simulation using an equivalent circuit representing the 2D multijunction FET, the "on" state of RTS appears when the photogenerated charge in the dot sensitively shifts the current level, while the on state returns to the "off" state when the charged dot is neutralized. The simulation result also shows that the RTS is triggered not only by the charging of a dot near the current percolation path, but also by the charging of a dot distances away from the path due to the nature of the multijunction system, i.e., the long screening length of the charge-induced potential. These results open up the development of single-photon devices with 2D multijunction systems.

I. INTRODUCTION

The detection of individual photons has attracted interest in the application to high sensitivity photodetectors as well as quantum cryptography. So far, photomultiplier tubes[1] and Si avalanche photodiodes[2,3] are widely used to detect the single photon, while visible light photon counters,[4,5] single-electron transistors,[6,7] and field-effect transistors (FET) containing quantum dots[8–11] are attractive as alternative methods. Previously, Shields *et al.*[8] have reported the detection of the single photon using $GaAs/Al_xGa_{1-x}As$ FET, in which the channel of two-dimensional electron gas is gated by a layer of InAs quantum dots separated by a thin $Al_xGa_{1-x}As$ barrier. In a very narrow channel, a single charge excited by the single-photon absorption and trapped in a dot sensitively alters the channel conductivity, leading to the single-photon detection. However, in this device, the active detection area is limited by the formation of the narrow channel, resulting in the narrow detection area ($<1~\mu m^2$). Therefore, for most of the practical device applications such as the photoimaging device,[12] an alternative device having a wide active area for the photon detection is inevitably required.

One approach to obtain a relatively wide detection area is to use a single-electron-tunneling device with a two-dimensional (2D) quantum dot array, such as 2D-dots-channel FET. This is because if each dot is connected to the gate via a sufficiently small capacitor, a current passing through the percolation path can be sensitively influenced by the change in the potential of the distant dots through multijunctions.[13,14]

In this paper, the carrier transport of 2D-Si-dots channel FET is shown to be modulated by the irradiation of photons. The transport modulation appears as the random telegraph signal (RTS) in the single-hole-tunneling characteristics. The individual RTS step is attributed to the single-photon absorption in the Si dots. A Monte Carlo simulation using an equivalent circuit consisting of 7×8 dots shows that, for a

sufficiently large screening length, the RTS is triggered not only by the single-photon-induced charging of the dots near the current percolation path, but also by the charging of the dots far from the path. This indicates that the 2D dots array system is effective for the application to the single-photon detector. In Sec. II, we first describe the device fabrication. In Sec. III, we then show the effects of light irradiation on the electrical characteristics of the device. In Sec. IV, we present and discuss the simulation result, which qualitatively agrees with the experimental result.

II. DEVICE FABRICATION

The device used for the experiments is the 2D-Si-multidot FET fabricated on a silicon-on-insulator (SOI) substrate,[15,16] as illustrated in Fig. 1(a). The channel widths and lengths are about 0.5 and 0.8 μm, respectively. In the channel, the Si single-crystalline dots are connected to each other via an ultrathin (about 5 nm) Si layer, which works as a tunnel barrier due to the quantum size effect. The 2D multidots are formed by the nanometer-scale local oxidation of Si (nano-LOCOS) process, which has mainly two steps.[15,17] First, the thin SOI surface was nitrided in a vacuum chamber to naturally form ultrasmall SiN islands. The initial thin SOI wafer is composed of a 18-nm-thick lightly doped *p*-type top Si (001) layer, a 90-nm-thick buried SiO_2 layer, and an n^+-type Si(001) substrate. Second, the surface was oxidized by a conventional furnace oxidation. Since the SiN islands work as the oxidation masks, Si multidots can be obtained below the SiN masks. From the atomic force microscope image, the lateral size, height, and density of the fabricated Si dots were found to be, on the average, 20 nm, 3 nm, and $2 \times 10^{11}~cm^{-2}$, respectively, although the size and spacing of the dots were distributed due to the naturally formed SiN masks. Here, the dots height of 3 nm is measured from the surface of the Si layer connecting the dots, so that the height
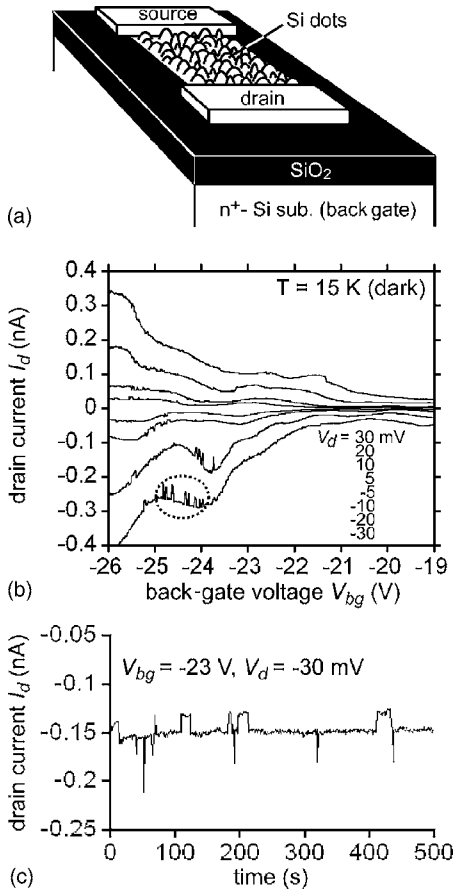
FIG. 1. (a) Schematic view of a 2D Si multidot channel FET, (b) I_d-V_{bg} of the single-hole characteristics for various V_d, and (c) I_d as a function of time at $V_{bg}=-23$ V and $V_d=-30$ mV.
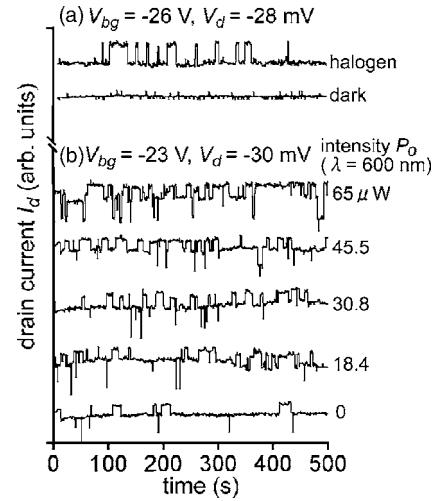

FIG. 2. (a) Time dependence of I_d for $V_{bg}=-26$ V and V_d $=-28$ mV in a dark condition and under a halogen lamp irradiation. (b) Time dependence of I_d for $V_{bg}=-23$ V and $V_d=-30$ mV in the dark condition and under light illumination with a wavelength λ of 600 nm for different light intensities P_o.

of the dots measured from Si/buried SiO$_2$ interface is about 8 nm.

In this work, the n^+-Si substrate is intentionally used as the back gate and no top gate is prepared in order to avoid the light absorption. The channel-source and channel-drain contacts are the Al Schottky contacts. The thickness of the Al electrodes is about 500 nm, which is thick enough to prevent the light penetration through the Al film. It is noted that the carriers are injected vertically at first through the Schottky barrier from the Al electrode to the Si channel by the back-gate-induced electric field, and then they are transported horizontally in the channel region by the source-drain voltage (V_d). Therefore, the light illumination effect should be absent at the Schottky contacts and present only in the multidot channel region. In addition, the carrier polarity can be selected by the polarity of the back-gate voltage (V_{bg}). For the positive V_{bg}, the electrons are injected into the channel and the FET acts as a single-electron device, while, for the negative V_{bg}, the holes are induced and the FET acts as a single-hole device.[15] The measurement temperature was 15 K.

III. DEVICE CHARACTERISTICS

Figure 1(b) shows the drain current (I_d) versus V_{bg} characteristics for the holes with different V_d in the dark condi-

tion. The current oscillations due to the Coulomb blockade (CB) effect are observed. As reported in our previous works,[15] the CB oscillations are ascribed to the formation of the 1D current percolation path, and a few dots having the highest resistance tunnel junctions in the path should dominate the carrier transport. A peculiar feature in the I_d-V_{bg} curves is a significant current noise as indicated by the dotted circle. In order to understand this feature, we observed the time dependence of I_d for $V_{bg}=-23$ V and $V_d=-30$ mV in the dark condition, as shown in Fig. 1(c). The current noise is found to be a discrete current switching between almost three current levels, i.e., the "off" state in the stationary state of about -0.15 pA and the "on" state in the other levels. Such a noise is known as the RTS. It has been reported previously that the RTS in the 2D Si dots system can be attributed to the charging-discharging of the dots adjacent to the current path.[18]

Figure 2(a) shows typical traces of I_d as a function of time for $V_{bg}=-26$ V and $V_d=-28$ mV in the dark condition and under a halogen lamp illumination. It is found that the RTS pattern with two digital current levels is clearly seen under the light illumination, while the RTS pattern is not seen in the dark condition. Such a photoinduced RTS was also clearly observed for other V_{bg} and V_d conditions, for example, as shown in Fig. 2(b). Figure 2(b) shows the time dependence of I_d for $V_{bg}=-23$ V and $V_d=-30$ mV under light illumination with a wavelength λ of 600 nm for different light intensities P_o. Hereafter, the number of on state in the RTS pattern per unit time is referred to as "frequency of RTS, N_{RTS}." In Fig. 2(b), N_{RTS} increases with P_o, i.e., the number of incident photons. It should be noted that the RTS pattern is observed even in the dark condition ($P_o=0$ μW) [see also Fig. 1(c)]. The time interval between the RTS events in the dark is of the order 1 min. The results in Figs. 2(a) and 2(b) strongly indicate that the generation of RTS in the current is triggered by the light illumination. Since the RTS in the dark may be due to the charging-discharging of
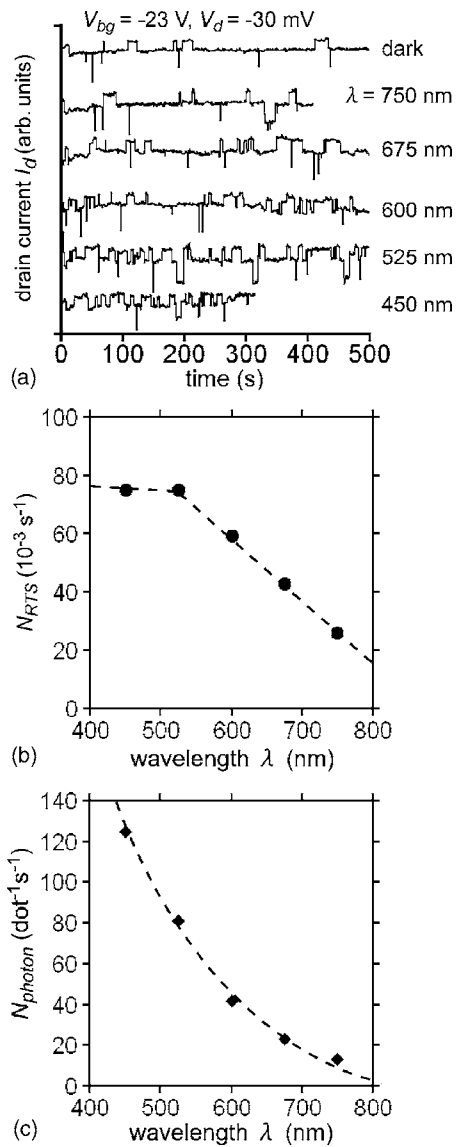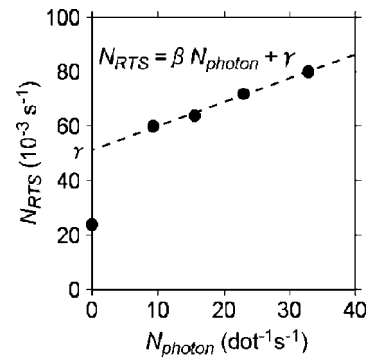
FIG. 4. Number of RTS events N_{RTS} as a function of the absorbed photons in the dots, N_{photon}, plotted from Fig. 2(b).

N_{RTS} increases with decreasing λ until λ of 500 nm and then saturates. This result indicates that N_{RTS} depends on the optical absorption coefficient of Si since the absorption coefficient increases with decreasing λ. We can estimate roughly the number of the absorbed photons in one Si dot, N_{photon}, using the following simple equation:[19]

$$N_{photon} = (\lambda/hc)(1 - R)[1 - \exp(-\alpha t_{dot})], \qquad (1)$$

where h is the Planck constant, c is the speed of light in vacuum, R is the Fresnel reflectance of Si surface, α is the absorption coefficient of the Si layer, and t_{dot} is the height of the Si dot. However, because of the multilayered structure, we need to take into account the effect of multiple internal reflection. Figure 3(c) shows N_{photon} as a function of λ taking the multiple internal reflection into account. N_{photon} is found to increase with decreasing λ, and this tendency qualitatively agrees with the behavior of N_{RTS} in Fig. 3(b) except for λ below 525 nm. This result indicates that RTS occurs due to the absorbed photons in the Si dots, although most of the incident photons pass through the dots because of the thin Si dots layer. Optimization of the device structure, such as introducing a multiple-absorption layer, is necessary to increase the photon absorption efficiency. The possible reason for the saturation of N_{RTS} for the shorter λ is that two or more charged dots are simultaneously generated but the change in the current level is dominated by one of the charged dots. This mechanism will be discussed in Sec. IV.

Next, we discuss the possible model for the generation of RTS. It is known that, in submicron channel Si metal-oxide-semiconductor field-effect transistors, the RTS occurs commonly due to the effect of interface states at Si/SiO₂.[20,21] In the 2D Si dots system, the charging-discharging of the dots becomes more crucial for the RTS because the multiple dots work as the trap sites.[18] The generation of RTS in Fig. 3 is likely to originate from the charging of the dots due to the light illumination. Figure 4 plots the number of RTS events (N_{RTS}), that corresponds to the number of single-photon absorption events, as a function of the absorbed photons in one dot (N_{photon}) from the experimental data in Fig. 2(b). The data show that N_{RTS} increases linearly with increasing N_{photon}. Here, a relationship between N_{RTS} and N_{photon} can be written as $N_{RTS} = \beta N_{photon} + \gamma$. The parameter β, the internal quantum efficiency, is 0.001, indicating that only a small
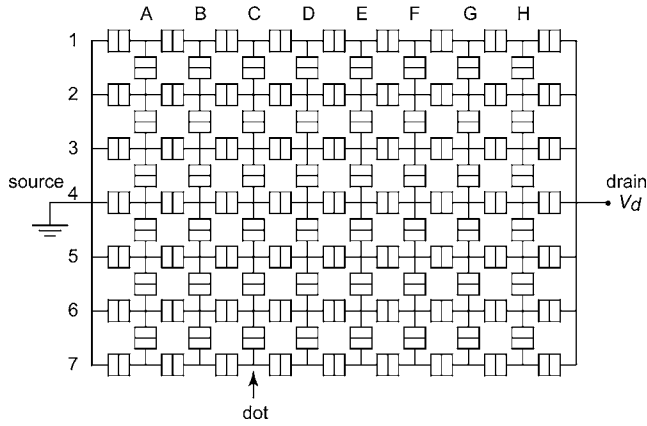

FIG. 3. (a) Time dependence of I_d under light illumination for different light wavelengths λ and (b) number of RTS events N_{RTS} as a function of λ. In this experiment, the incident photon flux is kept constant and estimated to be about 5.6×10^6 photons per second in the channel area (about 0.4 μm²). (c) Calculated number of the photons absorbed in one Si dot, N_{photon}, as a function of λ.

the dots adjacent to the current path due to a single-charge-tunneling from (to) the path to (from) the adjacent dots,[18] we believe that each current switching event under light illumination from the off state of RTS to the on state is due to the charging of individual dots in response to the trapping of a single photogenerated charge.

Next, the effect of photon absorption in the Si dots on the generation of RTS is investigated. Figure 3(a) shows the time dependence of I_d under light illumination for different λ. In this experiment, an incident photon flux is kept constant at 5.6×10^6 photons per second on the channel area (about 0.4 μm²). Taking into account that the number of the Si dots in the channel is about 20×25 dots, the incident photon flux directed to one dot is estimated to be 2200 photons per second. The N_{RTS} as a function of λ is shown in Fig. 3(b). The

FIG. 5. Equivalent circuit of the 2D tunnel junction array consisting of 7×8 dots used in the simulation. Each dot is connected to the gate voltage (V_g) through a gate capacitance (C_g).

fraction of absorbed photons trigger the RTS. Such photons initially generate the electron-hole pairs in the Si dots, leading to the charging of dots after the electron and hole are spatially separated by the electric field. As shown next by the simulation, if the photon is absorbed in the dot and its charging effect sensitively modulates the current, the on state of RTS can occur, while the off state will appear after the charged dot is neutralized.

On the other hand, most of the electron-hole pairs seem to immediately recombine in the same dot before both the carriers split, so that they do not induce the RTS. This problem will be solved by moderately increasing the applied gate voltage and the source-drain voltage to enhance the vertical and the horizontal electric field in the dot, as described in Sec. IV. It has been reported previously for the single-electron transistor with single Si dot (Coulomb island) that, the recombination of the electron-hole pair in the Si dot is avoided when the electric field in the dot is increased, resulting in the splitting of the electron and hole inside the Si dot.[22] It should be noted from Fig. 4 that the extraporated intercept γ is larger than the experimental value of $N_{RTS}(N_{photon}=0)$. Such a difference between the offset values may be caused by increasing the frequency of the charging and discharging events in the dots near the current path due to the photon-assisted tunneling.[23]

IV. A MONTE CARLO SIMULATION

As described above, the light illumination to the 2D Si dots FET leads to the generation of RTS in the current, indicating that the RTS is triggered by the single-photon absorption. In this section, we use an equivalent circuit consisting of 2D 7×8 dots array in Fig. 5, which represents the 2D multidot-channel FET, and we study the effect of light illumination on the current using a Monte Carlo simulation. Although the number of the dots used in this circuit is smaller than that of the actual dots in the channel (20×25 dots), the simulation result will be qualitatively the same. Each of the dots is connected to four neighboring dots in the vertical and horizontal directions through the small tunnel capacitance C
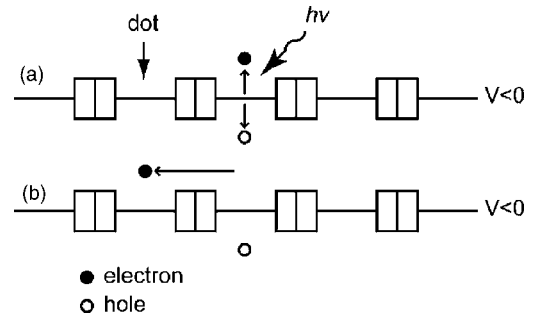

FIG. 6. (a) The photon induces the electron-hole pair in the Si dot; (b) the dot is charged after one type of the carriers leaves the other one due to an electric field.

with a tunnel resistance R_T and to a gate voltage source V_g through a gate capacitance C_g representing the buried SiO_2. The other capacitances between the distant dots are neglected. Since the size of the Si dots in the channel is distributed, the circuit parameters of C, C_g, and R_T are randomly varied. We set the values of C_i, C_{gj}, and R_{Ti} ($i=1 \sim 111$; $j=1 \sim 56$) in the ranges of 0.1 aF $\sim$ 1 aF, 0.04 aF $\sim$ 1 aF, and $4 \times 10^6 \ \Omega \sim 8.9 \times 10^{14} \ \Omega$; the average of 0.558 aF, 0.5582 aF, and $3.589 \times 10^{13} \ \Omega$; the standard deviations of 0.2878 aF, 0.2886 aF, and $1.475 \times 10^{14} \ \Omega$, respectively. All the tunnel resistances are larger than the quantum resistance $R_T \gg R_q = h/e^2$ and justify the use of the so-called orthodox theory of single-electron tunneling.

In this simulation, the light illumination effect is assumed as the charging of the dots, which occurs when the generated electron-hole pair [Fig. 6(a)] is separated from each other by an electric field, as shown in Fig. 6(b). Here, each photon is absorbed one-by-one randomly with time and in random dot locations. This assumption is based on the fact that the metallic dot system is used in the simulation, so that the generation of electron-hole pairs in the same dot cannot be included. However, it is noted that the splitting of the electron and hole can occur for the semiconductor dot, such as the Si dot.[22]

Next, we calculated the single-hole-tunneling characteristics of the circuit using a Monte Carlo method, ignoring cotunneling effects. The calculation is performed as follows.[24,25] First, the difference in the electrostatic energy of all the junctions before and after a tunneling event is estimated. Second, we calculate the forward and reverse tunneling rate $\Gamma^\pm$ at a junction using the following equation:[26]

$$\Gamma^\pm = \frac{1}{e^2 R_T} \frac{\Delta E^\pm}{[1 - \exp(-\Delta E^\pm / k_B T)]}, \qquad (2)$$

where e is an elemental charge, k_B is the Boltzmann constant, T is the temperature, and $\Delta E^\pm$ is the change in the total charging energy of the system due to the forward and reverse tunneling events. For simplicity, the temperature T is set to be 0 K, since even for finite temperature, the results are qualitatively the same for sufficiently small C and C_g. Therefore,
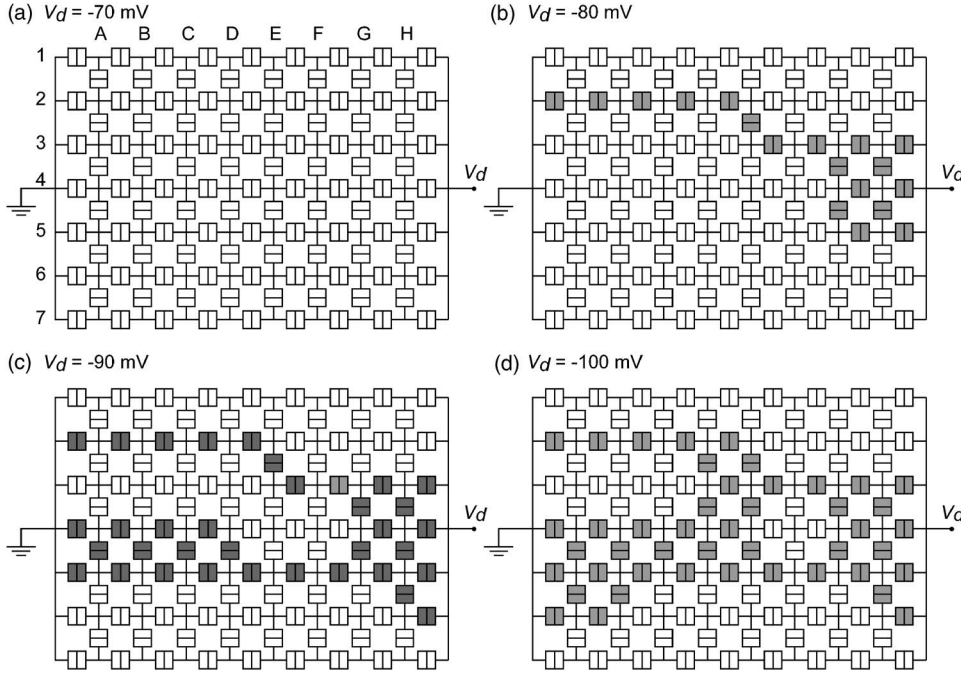
FIG. 7. Current percolation path in the dark condition at 0 K for $V_g=-15$ V and various V_d, i.e., (a) −70, (b) −80, (c) −90, and (d) −100 mV in the stationary state. The shaded tunnel junctions denote that the current flows through there.

$$\Gamma^\pm = 0 \text{ for } \Delta E^\pm < 0 \quad \text{and } \Gamma^\pm = \Delta E^\pm / e^2 R_T \text{ for } \Delta E^\pm > 0, \tag{3}$$

indicating that the single-charge tunneling is allowed only when the charging energy in the whole system is lowered by the tunneling. Third, the tunnel interval $u^\pm$ is calculated. Because $(\Gamma^\pm)^{-1}$ is the average interval between successive tunneling events, we simulated the tunneling intervals $u^\pm$ using a random number $r(0<r<1)$ by the following equation:

$$u^\pm = \frac{1}{\Gamma^\pm} \ln\left(\frac{1}{r}\right). \tag{4}$$

Here, the random number r is used to introduce the Stochastic nature of tunnel events in the Monte Carlo method. We calculate $u^\pm$ values for all the tunnel junctions, and choose a tunneling event with the minimum $u^\pm$, which is regarded as the tunneling that actually takes place. Then, we repeat the same procedure starting at $u^\pm$.

Figures 7(a)–7(d) show the current percolation path in the dark condition at 0 K for $V_g=-15$ V and various V_d, i.e., (a) −70, (b) −80, (c) −90, and (d) −100 mV in the stationary state. In these figures, the current only flows through the shaded tunnel junctions. At $V_d=-70$ mV [Fig. 7(a)], no current path is formed, indicating that the current is suppressed due to the Coulomb blockade effect. V_d is then increased to $V_d=-80$ mV, which is just above the threshold voltage. At this condition, nearly a single current path is formed, as shown in Fig. 7(b). Here, the single-hole-tunneling current flows from the source to the drain through the one-dimensional dots array of the current path except for the area near the drain electrode. When V_d is further increased to −90 and −100 mV, as shown in Figs. 7(c) and 7(d), respectively, branches or new percolation paths are formed. The similar current path has been reported for the 2D array of small

metallic dots with random offset charges on each dot, where the single current path with few or no branches is found at the voltage just above threshold.[27]

Figure 8(a) shows the calculated current as a function of time at $V_g=-15$ V and $V_d=-80$ mV in the dark condition and under light illumination. To avoid the effect of individual single-charge-tunneling (SCT) event on the current, we choose an appropriate integration time on the order of micro-
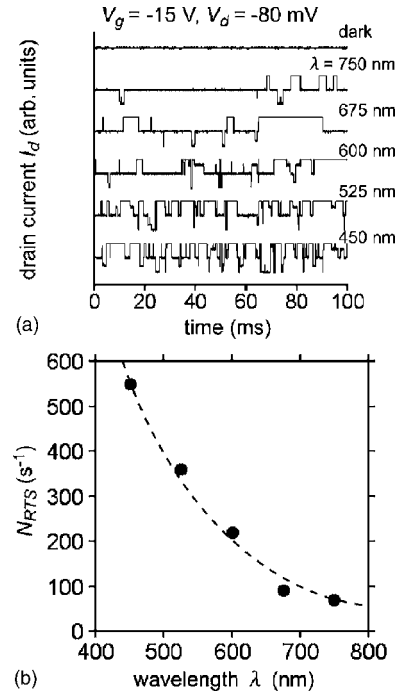

FIG. 8. (a) Calculated current as a function of the time at $V_g=-15$ V and $V_d=-80$ mV in the dark condition and under light illumination and (b) the number of RTS events N_{RTS} as a function of the light wavelength λ plotted from 8(a).
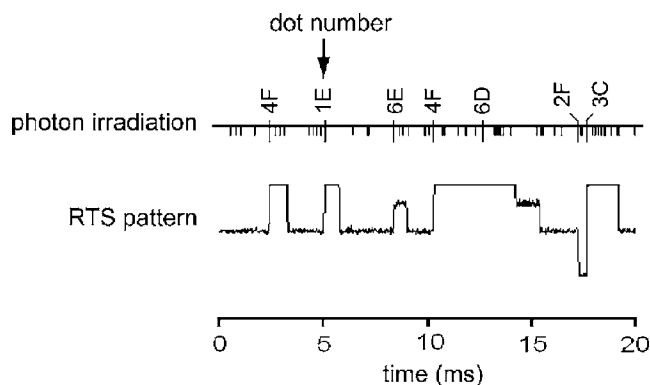
FIG. 9. Typical RTS pattern for wavelength $\lambda = 525$ nm and the time of photon illumination. Numbers of $1E$, $2F$, $3C$, $4F$, $6D$, and $6E$, denote the dot numbers which induce the RTS. The dot number is defined in Fig. 5.

seconds, which is larger than the tunneling interval of SCT events (<1 nanosecond). The light illumination effect on the current is calculated using the absorbed photon flux of 125, 81, 42, 23, and 13 photons per second in one dot. These numbers of photons are equal to those for the experiments with the wavelengths λ of 450, 525, 600, 675, and 750 nm, respectively. As a result, the RTS pattern is clearly seen under the light illumination, while the RTS is absent in the dark condition. The number of RTS events (N_{RTS}) as a function of the light wavelength from the simulation result in Fig. 8(a) is shown in Fig. 8(b). It is seen that N_{RTS} increases with decreasing λ. These simulation results qualitatively reproduce the experimental results in Fig. 3.

In order to understand the origin of RTS in Fig. 8(b), we discuss the relationship between the time of RTS events and that of the photon absorption in the dots. Figure 9 shows the typical RTS pattern for the wavelength $\lambda = 525$ nm, including the time of the photon absorption event on top. The dots, which cause the on state of RTS, are denoted by the dot number, as defined in Fig. 5. It is found that the on state of RTS appears when the photons are absorbed in the dots with the dot sites of $1E$, $2F$, $3C$, $4F$, $6D$, and $6E$, while the RTS pattern is absent when the photons are absorbed in the other ones. Such active dots are not limited to the vicinity of the current path. In fact, distant dots such as $6D$ and $6E$ also generate the on state of RTS. It is also found that the residence time τ of the photoexcited charge in these dots is equal to the duration of the on state RTS. These results indicate that the absorbed photons in the dot induces the on state of RTS, while the off state appears when such a charged dot is neutralized. The neutralization of the charged dot occurs when the photocarrier leaves the dot, or when the other different types of carriers enter in the charged dot. However, it should be noted that, only the dots, having the larger τ than integration time, sensitively induce the RTS.

In addition, Fig. 9 also shows that two active dots, i.e., $4F$ and $6D$, are present in the same time range of 10–14 ms. It can be seen that dot $4F$ readily becomes an active dot to cause the on state, while the effect of charging in dot $6D$ appears only after the dot $4F$ is neutralized. This indicates that the dot having the strongest charging effect dominantly induces the RTS if two or more active dots appear simultaneously. This may be the reason why the frequency of RTS in Fig. 3(b) saturates with decreasing the light wavelength.

Next, three important factors, which play a key role in the generation of RTS, are discussed. The *first one* is the screening length in the multijunction system, which determines whether the distant dots sensitively induce the RTS or not. From Fig. 9, the RTS is triggered not only by the charging of the dots adjacent to the current path, but also by that of the dots away from the path. The screening length Λ is proportional to $(C/C_g)^{1/2}$,[13] where C/C_g is a ratio of the tunnel capacitance C to the gate capacitance C_g. It is found that the charging of the dots away from the current path sensitively induces the RTS when the value of Λ is large. For example, when we use the circuit with constant values of C and C_g, which give for $\Lambda > 7$, the current path is sensitively influenced even by the charging of the dot, that is furthest away from the path. This indicates that the effect of charged dots on the generation of RTS should be stronger for smaller C_g. This may be because the changes in the electric potential will be easily transmitted from the charged dot away from the path into the current path for small C_g. Based on this analysis, in order to fabricate the wide detection area device using 2D dots array system, a small value of C_g is required. In our device, C and C_g are estimated to be about 0.2–0.5 aF and 0.5–1.1 aF, respectively, so that the Λ is estimated to be about 0.4–1.0. This value is smaller, compared with the estimated value above, suggesting that RTS in Figs. 2 and 3 is mainly attributed to the charging of the dots near the current path.

The *second important factor for* RTS is the residence time τ of the photoinduced charge in the dot. In order to observe the RTS pattern, τ is required to be larger than the integration time. According to Eq. (4), τ depends on the tunneling rate, which is expressed using the charging energy and the tunnel resistance (R_T) surrounding the dot [see Eq. (2)]. If the charging energy of the whole system is lowered by the trapping of one photocharge in the dot due to the absorption of the photon, the photocharge will be stable in the dot. Considering that the charging energy is inversely proportional to the capacitance, the long τ is obtained for the large dot capacitance C_{dot}. Additionally, since τ is also proportional to R_T, the long τ is obtained when the large R_T surrounds the dot. It should be noted that, although both C_{dot} and R_T influence τ, C_{dot} is more dominant than R_T in the single-electron-tunneling orthodox theory.[26] This is because the tunneling event depends on the change in the charging energy of the whole system [see Eq. (3)].

The *third one* is the splitting of the photogenerated electron-hole pair. As mentioned in Sec. III, the charging of the dots, which is the origin of RTS, occurs if the photogenerated electron-hole pair is splitted. The splitting process can be enhanced by the combination of applying back-gate voltage and source-drain voltage, i.e., the electron-hole pair is splitt vertically in the dot at first by applying the back-gate voltage, preventing them from recombination,[22] and then they are separated from each other horizontally by the source-drain voltage.

Finally, it is obvious that the charging effect in the 2D dots array system due to the light illumination plays a key

role in the generation of RTS from the comparison between the experiment and simulation with the smaller-scale 2D circuit. However, there are differences in the detail of RTS patterns between the experiment and the simulation, such as the duration time of RTS and the fine structure of RTS. To explain quantitatively the RTS patterns in Figs. 2 and 3, we have to extend the simulation using the circuit consisting of the dots array with the larger dot number and appropriate circuit parameters reflecting the fabricated device. Additionally, the simulation result also suggests that the 2D dots array system can be applied to the single-photon detector, where the channel area of 2D dots array can be significantly increased in the horizontal direction, while keeping the screening length sufficiently large. However, in order to increase the quantum efficiency in the vertical direction, optimization and reconstruction of the whole device structure such as introducing a multiple-absorption layer are required.

V. CONCLUSIONS

We have demonstrated the single-photon detection using 2D Si multidot channel FET. We found that the light illumination induces the generation of RTS, where the frequency of RTS events depends on the light wavelength and intensity.

This result indicates that RTS is triggered by the single-photon absorption in the Si dots. A Monte Carlo simulation using an equivalent 2D circuit consisting of 7×8 dots shows that the on state of RTS appears when the photon is absorbed in the dot and its charging effect influences the current, while the off state of RTS appears when the charged dot is neutralized. It is also found that, for sufficiently large screening lengths, RTS is triggered not only by the charging of the dots adjacent to the current percolation path, but also by the charging of the dots away from the path. These results provide a possibility of developing the single-photon detector using 2D dots system.

ACKNOWLEDGMENTS

*Electronic address: romtabe@rie.shizuoka.ac.jp

[1] R. S. Bondurant, P. Kumar, J. H. Shapiro, and M. M. Salour, Opt. Lett. **7**, 529 (1982).

[2] H. Dautet, P. Deschamps, B. Dion, A. D. MacGregor, D. MacSween, R. J. McIntyre, C. Trottier, and P. P. Webb, Appl. Opt. **32**, 3894 (1993).

[3] P. G. Kwiat, A. M. Steinberg, R. Y. Chiao, P. H. Eberhard, and M. D. Petroff, Phys. Rev. A **48**, R867 (1993).

[4] M. D. Petroff, M. G. Stapelbroek, and W. A. Kleinhans, Appl. Phys. Lett. **51**, 406 (1987).

[5] J. Kim, Y. Yamamoto, and H. H. Hogue, Appl. Phys. Lett. **70**, 2852 (1997).

[6] A. N. Cleland, D. Esteve, C. Urbina, and M. H. Devoret, Appl. Phys. Lett. **61**, 2820 (1992).

[7] S. Komiyama, O. Astafiev, V. Antonov, T. Kutsuwa, and H. Hirai, Nature (London) **403**, 405 (2000).

[8] A. Shields, M. P. O'Sullivan, I. Farrer, D. A. Ritchie, R. A. Hogg, M. L. Leadbeater, C. E. Norman, and M. Pepper, Appl. Phys. Lett. **76**, 3673 (2000).

[9] H. Kosaka, D. S. Rao, H. D. Robinson, P. Bandaru, T. Sakamoto, and E. Yablonovitch, Phys. Rev. B **65**, 201307(R) (2002).

[10] G. Yusa and H. Sakaki, Appl. Phys. Lett. **70**, 345 (1997).

[11] J. J. Finley, M. Skalitz, M. Arzberger, A. Zrenner, G. Bohm, and G. Abstreiter, Appl. Phys. Lett. **73**, 2618 (1998).

[12] M. Tabe, Y. Terao, R. Nuryadi, Y. Ishikawa, N. Asahi, and Y. Amemiya, Jpn. J. Appl. Phys., Part 1 **38**, 593 (1999).

[13] J. E. Mooij and Gerd Schön, in *Single Charge Tunneling*, edited by H. Grabert and M. H. Devoret (Plenum Press, New York, 1992), p. 277.

[14] K. K. Likharev, N. S. Bakhvalov, G. S. Kazacha, and S. I. Serdyukova, IEEE Trans. Magn. **25**, 1436 (1989).

[15] R. Nuryadi, H. Ikeda, Y. Ishikawa, and M. Tabe, IEEE Trans. Nanotechnol. **2**, 231 (2003).

[16] H. Ikeda, R. Nuryadi, Y. Ishikawa, and M. Tabe, Jpn. J. Appl. Phys., Part 1 **43**, L759 (2004).

[17] M. Tabe, M. Kumezawa, T. Yamamoto, S. Makita, T. Yamaguchi, and Y. Ishikawa, Appl. Surf. Sci. **142**, 553 (1999).

[18] R. Nuryadi, H. Ikeda, Y. Ishikawa, and M. Tabe, Appl. Phys. Lett. **86**, 133106 (2005).

[19] S. M. Sze, *Physics of Semiconductor Devices*, 2nd ed. (Wiley, New York, 1981), p. 756.

[20] M. Bollu, F. Koch, A. Madenach, and J. Scholz, Appl. Surf. Sci. **30**, 142 (1987).

[21] A. Neugroschell, C. T. Sah, and M. S. Carroll, Appl. Phys. Lett. **66**, 2879 (1995).

[22] A. Fujiwara, Y. Takahashi, and K. Murase, Phys. Rev. Lett. **78**, 1532 (1997); A. Fujiwara, K. Yamazaki, and Y. Takahashi, Appl. Phys. Lett. **80**, 4567 (2002).

[23] L. P. Kouwenhoven, S. Jauhar, K. McCormick, D. Dixon, P. L. McEuen, Yu. V. Nazarov, N. C. van der Vaart, and C. T. Foxon, Phys. Rev. B **50**, R2019 (1994).

[24] M. Tabe, N. Asahi, Y. Amemiya, and Y. Terao, Jpn. J. Appl. Phys., Part 1 **36**, 4176 (1997).

[25] M. Tabe, Y. Terao, N. Asahi, and Y. Amemiya, IEICE Trans. Electron. **E81-C**, 36 (1998).

[26] M. H. Devoret and H. Grabert, in *Single Charge Tunneling*, edited by H. Grabert and M. H. Devoret (Plenum Press, New York, 1992), p. 12.

[27] A. A. Middleton and N. S. Wingreen, Phys. Rev. Lett. **71**, 3198 (1993).